DETECTION OF PERINATAL HYPOXIA USING TIME–FREQUENCY ANALYSIS OF HEART RATE VARIABILITY SIGNALS

Shiying Dong[1], Boualem Boashash[1,2], Ghasem Azemi[1], Barbara E. Lingwood[1], and Paul B. Colditz[1]

[1]The University of Queensland, UQ Centre for Clinical Research, Herston QLD, Australia
[2]College of Engineering, Qatar University, Qatar

ABSTRACT

This paper presents a time–frequency approach to detect perinatal hypoxia by characterizing the nonstationary nature of heart rate variability (HRV) signals. Quadratic time–frequency distributions (TFDs) are used to represent the HRV signals. Six features based on the instantaneous frequency (IF) of the lower frequency components of HRV signals are selected to establish a classifier using support vector machine. The classifier is trained and tested using the signals recorded from a neonatal piglet model under a controlled hypoxic condition, which provides reliable annotations on the data. The method shows superior performance in the detection of hypoxic epochs with sensitivity (89.8%), specificity (100%) and total accuracy (94.9%) compared with that based on frequency domain features, indicating that nonstationarity should be taken into account for a more accurate assessment of the newborn status with possible hypoxia when analyzing HRV signals.

Index Terms— time–frequency distribution, heart rate variability, nonstationarity, perinatal hypoxia

1. INTRODUCTION

Perinatal hypoxia, occurring due to a variety of events such as antepartum maternal hypotension and intrapartum placental abruption, is a major cause of cerebral injury, accounting for a large amount of morbidity and mortality in neonates [1]. Early detection of hypoxia is of great clinical importance to reduce the risk of adverse outcomes following the insult. Moreover, it may help clinicians plan and conduct appropriate therapeutic strategies promptly to prevent or alleviate the consequent brain injury.

Current approaches for hypoxia detection in the fetus depend primarily on the analysis of cardiotocography (CTG) [2]. This method is based on visual pattern recognition of trended data by trained clinicians, but has high inter- and intra-observer variability due to subjectivity [3]. This has led to sufficient motivation to explore automated and objective approaches to detecting hypoxia [2].

Heart rate variability (HRV) signals are defined as the variation of inter-heartbeat intervals. Since these signals can be non-invasively monitored, they have drawn much attention in designing effective detection methods for perinatal hypoxia. Frequency domain analysis of HRV signals provides recognized features as assessment of the neurological cardiovascular regulation [4]. Fast Fourier transform and autoregression methods are predominately used in estimating the spectral features such as the power within bands of clinical significance. Clinical studies have shown that these features are indicative of hypoxic insult but with a low specificity [6], which may cause unnecessary interventions without improvement in fetal outcome [3]. Other studies on automated methods for hypoxia detection involve other HRV features such as nonlinear indices [7], [8] and system model parameters [9].

Nonstationarity is a natural characteristic of HRV signals and therefore, without carefully controlling the experimental conditions, the HRV features may be significantly contaminated by nonstationarity [11]. This fact may be the potential reason for the low specificity of hypoxia detection methods which use frequency domain features of HRV signals. Despite this, the stationary methods still prevail in clinical research and practice due to their widely-accepted physiological relevance (where assuming the signals are stationary or at least quasi-stationary) [4]. It has also been the case in the study of perinatal hypoxia detection.

Taking the nonstationarity of HRV signals into account, wavelet analysis has been used to estimate the scale-dependent coefficients as part of the feature set in combination with fetal pulse oximetry ($FSpO_2$) [10]. In [12], empirical mode decomposition was used to extract features of nonstationary characteristic; however, these features are not of definite physiological relevance.

Quadratic time–frequency distributions (TFDs) represent the signal energy distribution simultaneously in both time and frequency domains, and capture the nonstationarity of multi-component signals, such as HRV, as well as provide a simple and accurate way to estimate instantaneous frequency (IF) [13]. TFDs have been widely used in HRV analysis due to these advantages [14], but have not yet been applied in feature extraction for hypoxia detection. Therefore, TFDs are used in the present study to estimate the IF and associated features, which are then applied in building the classifier for hypoxia detection.

Herein, we present an automatic hypoxia detection method using TFD-based features extracted from HRV

signals. The features are classified using a support vector machine. The method is trained and tested using the data collected from a piglet model.

2. HRV DATA AND TFD-BASED METHODS

2.1. Experiment, data recording and pre-processing

In this study, we used 21 neonatal piglets under hypoxic condition to simulate perinatal hypoxia in human babies. This approach has been used widely in the pathophysiological studies of perinatal hypoxia because piglets have similar ontogenesis of nervous and cardiovascular systems to human babies [15]. On the other hand, although newborn HRVs have been used to explore effective hypoxia detection methods, a big concern is the annotation of the data. The class of the data (normal/abnormal) is generally determined either by expert annotation according to CTG analysis guidelines or by umbilical artery blood pH or base deficit measured right after delivery [8], [12]. The first approach is considered subjective due to the inter- and intra-observer variability [3], while the second method has no consensus on the threshold of blood pH or base deficit separating the classes, which is a major uncertainty that affects the detection performance [7]. In contrast, the animal model experiment using controlled hypoxia enables a definite and accurate annotation of the data, guaranteeing the effectiveness of the proposed method.

In this experiment, the piglets were anaesthetized and continuously monitored. The respiration of the animals was controlled using a neonatal ventilator at a rate of 30 breaths per minute (BPM). Hypoxia was induced by lowering the fraction of inspired oxygen (FiO_2) to 0.1 for 30 minutes. A detailed description of the experiment can be found in [15].

Electrocardiogram (ECG) signals for HRV analysis were recorded with Powerlab (ADInstruments, Sydney, Australia) at a rate of 1 kHz. All the following signal processing was implemented using MATLAB (Version R2011b, Mathworks Inc, Natick, MA). A 5 minutes epoch of ECG before and at the beginning of the hypoxic insult were converted to HRV signals as follows: A Hilbert transform-based method was first used to locate the R-peaks and then HRV signals were generated accordingly [18]. The outliers were removed and the resulting signals resampled at 4 Hz by cubic spline interpolation. The mean value and linear trend were subtracted from the resampled signals. The first 1024 samples (≈4.27 minutes) were used for TFD analysis. This data size was chosen because it is not only suitable for fast processing but also close to the required time duration for the identification of hypoxia that is of prognostic significance and needs clinical intervention [2].

2.2. Time–frequency analysis of HRV signals

Time–frequency distributions have been widely used in characterizing time-varying multi-component signals, such as HRV. Given an analytic signal $z(t)$, the general form of a quadratic TFD $\rho_z(t,f)$ can be expressed as [13]:

$$\rho_Z(t,f) = \int\int G(t-u,\tau)\, z\left(u+\frac{\tau}{2}\right) z^*\left(u-\frac{\tau}{2}\right) e^{-j2\pi f\tau} du d\tau \quad (2)$$

where $G(t,\tau)$ is a time-lag kernel, used to suppress the cross-terms generated as a result of the quadratic nature of TFD, and * represents complex conjugation. Among a variety of TFDs in the literature, the spectrogram and modified B-distribution (MBD) have shown high quality in the representation of HRV signals in terms of resolution preservation and cross-term reduction [19], whereas the TFD with the compactly supported separable Gaussian kernel (CSSGD) is a most recently proposed TFD with good performance [16]. In this study, we compare these TFDs in characterizing piglet HRV signals according to the consequent hypoxia detection outcomes. Table 1 lists the formulas of these kernels in time-lag domain and their parameters used in the analysis.

Table 1: TFD kernels in the time-lag domain.

TFD	Kernel $G(t,\tau)$	Parameters
Spectrogram	$w(t+\frac{\tau}{2})w(t-\frac{\tau}{2})$	Hanning window, Size = 75
MBD	$\frac{cosh^{-2\beta}(t)}{\int cosh^{-2\beta}(\zeta)d\zeta}$	β = 0.03
CSSGD	$e^{2C+\frac{CD^2}{\tau^2-D^2}} \int_{-\infty}^{\infty} e^{\frac{CD^2}{v^2-D^2}} e^{-j2\pi tv} dv$	C = 2, D = 15

2.3. Time–frequency feature extraction and selection

There are three components that are generally recognized in HRV. The high frequency (HF) component reflects the vagally-mediated respiratory sinus arrhythmia; the low frequency (LF) is associated with both sympathetic and vagal regulation; and the very low frequency (VLF) is linked to various neural and hormonal effects. We defined the frequency bands of interest as VLF (0-0.02 Hz), LF (0.02-0.1 Hz) and HF (0.45-0.55 Hz), where the power is most concentrated [17]. Fig.1 illustrates the representation of piglet HRV epochs under hypoxic and non-hypoxic conditions using the MBD.

We used the IF of each component as the dynamic feature and estimated them by means of the local maxima from the time–frequency representation. Given a temporal slice in the TFD, the IF was estimated by [5]:

$$\hat{f}_i^{(m)}(t) = arg\left\{\max_f \rho_z(t,f)\right\}, \quad m \in \{VLF, LF, HF\} \quad (5)$$

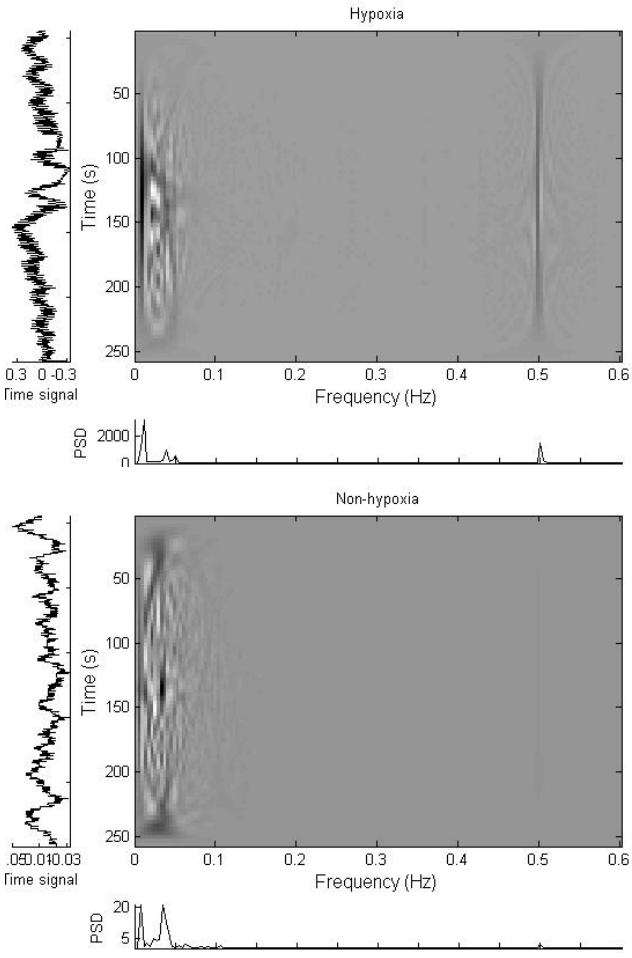

Fig.1: MBD ($\beta = 0.03$) of piglet HRV epochs under hypoxic and non-hypoxic conditions.

where m denotes the component. Another feature based on the IF is the local maximal value of TFD at the IF $\hat{f}_i^{(m)}(t)$, calculated as:

$$\hat{p}_i^{(m)}(t) = \rho_z\left(t, \hat{f}_i^{(m)}(t)\right), m \in \{VLF, LF, HF\} \qquad (6)$$

The mean and standard deviation of $\hat{f}_i^{(VLF)}$, $\hat{f}_i^{(LF)}$, $\hat{p}_i^{(VLF)}$, $\hat{p}_i^{(LF)}$ and $\hat{p}_i^{(HF)}$ over time were calculated as potential features. Since the respiration rate remained constant at 0.5 Hz (equivalent to the ventilation rate at 30 BMP), the HF component (*i.e.* $\hat{f}_i^{(HF)}$) was constantly equal to 0.5 Hz throughout the experiment; thus only $\hat{p}_i^{(HF)}$ was taken into consideration. We only considered these simple statistical nonstationary features to investigate the potentiality of time–frequency analysis in designing effective hypoxia detection approach in this preliminary study. More sophisticated features will be taken into account in future studies.

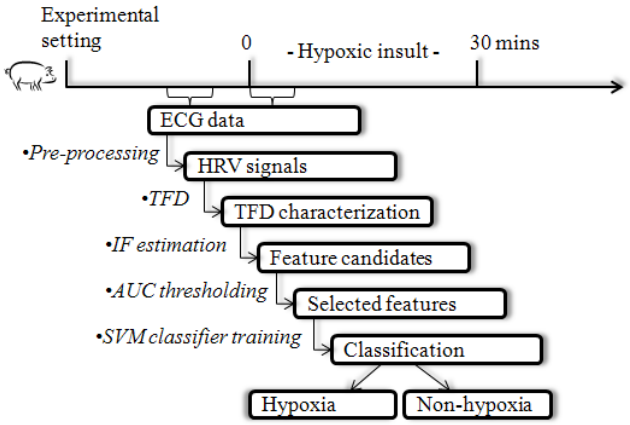

Fig. 2: Diagram of the proposed hypoxia detection method.

In order to make a complete and fair comparison between the frequency domain approach and the time–frequency approach, the following features were extracted from the frequency domain representation. The power spectral density (PSD) of HRV epochs was obtained using Fast Fourier transform and the power in the three bands as previously defined was computed. The normalized power for three components and the ratio of LF over HF, according to the standard [4], were calculated as the features to be fed into the classifier.

To select the most effective features, the receiver operating characteristics (ROC) was used to assess the capability of discriminating hypoxic epochs from the non-hypoxic epochs, and the area under the ROC curve was used as a metric. We selected the best 6 features to construct the classifier by setting the AUC threshold as 85% out of the unit area.

2.4. Classification

Support vector machine (SVM) was used to establish the classifier based on the selected features, as it has been used with success in most studies of automated hypoxia detection methods [7]–[9]. Moreover, it makes our results comparable with theirs from the perspective of classifier. Three kernel functions were considered in this work, which were quadratic kernel, polynomial kernel and Gaussian radial basis function (GRBF) kernel respectively. Regarding the parameter setting, the polynomial kernel came with the order equal to 3, and the scaling factor in GRBF kernel was chosen as 1. The hyperplane separating the two classes were found by least squares method.

The diagram of the proposed hypoxia detection method is illustrated in Fig.2.

3. RESULTS AND DISCUSSION

Considering the limited dataset, we performed 7-fold cross-validation randomly on the dataset with 50 iterations.

Results presented are the averaged values of all iterations. Sensitivity, specificity and accuracy were used as criteria to evaluate the performance of the proposed hypoxia detection method.

In the feature selection, the best 6 features for the threshold AUC>85% consist of the mean and standard deviation of $\hat{p}_i^{(VLF)}$, $\hat{p}_i^{(LF)}$ and $\hat{f}_i^{(VLF)}$ for all TFDs. As an example, the AUC results for the features using MBD are tabulated in Table 2. The effective features are derived from VLF and LF component, indicating a significant change in the lower frequency bands regulated by both sympathetic and parasympathetic nervous systems.

With respect to the classifier, the results show that the SVM with quadratic kernel is best-suited to PSD features (Table 3). In contrast, the GRBF kernel outperforms the other kernel functions in building the SVM classifier with superior overall outcomes based on TFD features (Table 3), which is in agreement with the result in the literature [7]–[9].

Regarding the detection results, the TFD features show higher performance compared with PSD features in general (Table 3). Specifically, MBD-based features combined with the SVM classifier of GRBF kernel have the best performance in general with 89.8% in sensitivity, 100% in specificity and 94.9% in accuracy. Apart from the effectiveness of SVM kernel, this may also be accounted for by the lag-independent kernel of MBD, which is more accurate in characterizing the temporally slowly-varying components of HRV signals than the kernels of the other TFDs [13], [19]. The results also demonstrate that the proposed method may not only detect the hypoxic insult with a high accuracy but also effectively avoid false positive detections, which may reduce unnecessary clinical management that could cause adverse side effects.

In comparison of feature effectiveness with other proposed methods, conventional frequency domain features of HRV have been used together with time domain features [7], parameters from CTG system model [9] and nonlinear indices [8]. Although these features show a certain degree of effectiveness, failure in considering the nonstationary nature of HRV signals may be a reason of the relatively low sensitivity, specificity and accuracy.

4. CONCLUSION

Accurate detection of perinatal hypoxia plays a significant role in reducing the risk of neonatal brain injury. In this study, we propose a hypoxia detection method using a SVM classifier with TFD-based features extracted from HRV signals. Tested using the data recorded from a piglet model under controlled hypoxic condition, the method shows high sensitivity, specificity and accuracy in the detection. The result also indicates that nonstationarity should be considered in assessing the newborn status with possible hypoxia when using HRV signals. In future work, TFDs with better TF resolution and IF estimation methods with higher accuracy will be applied to improve the detection performance [19]. On the other hand, the proposed method needs to be tested on accurately labeled data from human neonates to become clinically applicable in hypoxia detection.

Table 2: The AUC values for MBD-based features (std stands for standard deviation).

Feature	AUC (%)	Feature	AUC (%)
mean$\{\hat{p}_i^{(VLF)}\}$	99.3*	mean$\{\hat{f}_i^{(VLF)}\}$	90.3*
std$\{\hat{p}_i^{(VLF)}\}$	98.9*	std$\{\hat{f}_i^{(VLF)}\}$	89.6*
mean$\{\hat{p}_i^{(LF)}\}$	99.8*	mean$\{\hat{f}_i^{(LF)}\}$	73.7
std$\{\hat{p}_i^{(LF)}\}$	99.3*	std$\{\hat{f}_i^{(LF)}\}$	78.5
mean$\{\hat{p}_i^{(HF)}\}$	77.3		
std$\{\hat{p}_i^{(HF)}\}$	76.6		

* Selected features for classifier construction.

Table 3: Detection results for SVM classifiers with PSD and different TFD features.

SVM	Index	PSD	Spectrogram	MBD	CSSGD
Quadratic	Sensitivity (%)	84.7	75.7	77.9	81.3
	Specificity (%)	82.3	95.3	98.3	99.9
	Accuracy (%)	83.5	85.5	88.1	90.6
Polynomial	Sensitivity (%)	84.4	77.2	88.0	85.9
	Specificity (%)	77.0	95.5	99.8	99.4
	Accuracy (%)	80.7	86.4	93.9	92.7
GRBF	Sensitivity (%)	81.3	87.2	**89.8**	90.5
	Specificity (%)	82.8	95.2	**100**	95.2
	Accuracy (%)	82.0	91.2	**94.9**	92.9

5. REFERENCES

[1] D.M. Ferriero, "Neonatal brain injury," *New England Journal of Medicine*, vol. 351, no. 19, p. 1985, 2004.

[2] G.A. Macones, G.D. V. Hankins, C.Y. Spong, J. Hauth, and T. Moore, "The 2008 National Institute of Child Health and Human Development workshop report on electronic fetal monitoring: update on definitions, interpretation, and research guidelines," *Obstetrics & Gynecology*, vol. 112, no. 3, pp. 661–666, 2008.

[3] Z. Alfirevic, D. Devane, and G.M.L. Gyte, "Continuous cardiotocography (CTG) as a form of electronic fetal monitoring (EFM) for fetal assessment during labour," *Cochrane Database of Systematic Reviews*, vol. 3, 2006.

[4] Task Force of the European Society of Cardiology and the North American Society of Pacing and Electrophysiology, "Heart rate variability: standards of

measurement, physiological interpretation, and clinical use," *Circulation*, vol. 93, no. 5, pp. 1043–1065, 1996.

[5] S. Dong, G. Azemi, B. Lingwood, P.B. Colditz, and B. Boashash, "Performance evaluation of multi-component instantaneous frequency estimation techniques for heart rate variability analysis," in *11th International Conference on Information Science, Signal Processing and their Applications (ISSPA)*, pp. 1211–1216, 2012.

[6] J. Van Laar, M.M. Porath, C.H.L. Peters, and S.G. Oei, "Spectral analysis of fetal heart rate variability for fetal surveillance: review of the literature," *Acta Obstetricia et Gynecologica*, vol. 87, no. 3, pp. 300–306, 2008.

[7] G. Georgoulas, D. Stylios, and P. Groumpos, "Predicting the risk of metabolic acidosis for newborns based on fetal heart rate signal classification using support vector machines," *IEEE Transactions on Biomedical Engineering*, vol. 53, no. 5, pp. 875–884, 2006.

[8] J. Spilka, V. Chudáček, M. Koucký, L. Lhotská, M. Huptych, P. Janků, G. Georgoulas, and C. Stylios, "Using nonlinear features for fetal heart rate classification," *Biomedical Signal Processing and Control*, vol. 7, no. 4, pp. 350–357, 2012.

[9] P.A. Warrick, E.F. Hamilton, D. Precup, and R.E. Kearney, "Classification of normal and hypoxic fetuses from systems modeling of intrapartum cardiotocography," *IEEE Transactions on Biomedical Engineering*, vol. 57, no. 4, pp. 771–779, 2010.

[10] E. Salamalekis, P. Thomopoulos, D. Giannaris, I. Salloum, G. Vasios, A. Prentza, and D. Koutsouris, "Computerised intrapartum diagnosis of fetal hypoxia based on fetal heart rate monitoring and fetal pulse oximetry recordings utilising wavelet analysis and neural networks," *BJOG: An International Journal of Obstetrics and Gynaecology*, vol. 109, no. 10, pp. 1137–1142, 2002.

[11] V. Magagnin, T. Bassani, V. Bari, M. Turiel, R. Maestri, G.D. Pinna, and A. Porta, "Non-stationarities significantly distort short-term spectral, symbolic and entropy heart rate variability indices," *Physiological Measurement*, vol. 32, p. 1775, 2011.

[12] N. Krupa, M. Ali, E. Zahedi, S. Ahmed, and F.M. Hassan, "Antepartum fetal heart rate feature extraction and classification using empirical mode decomposition and support vector machine," *Biomedical Engineering Online*, vol. 10, p. 6, 2011.

[13] B. Boashash, *Time Frequency Signal Analysis and Processing: A Comprehensive Reference*. Oxford, UK: Elsevier, 2003.

[14] L.T. Mainardi, "On the quantification of heart rate variability spectral parameters using time–frequency and time-varying methods," *Philosophical Transactions of the Royal Society A: Mathematical, Physical and Engineering Sciences*, vol. 367, no. 1887, p. 255, 2009.

[15] S.T. Bjorkman, K.A. Foster, S.M. O'driscoll, G.N. Healy, B.E. Lingwood, C. Burke, and P.B. Colditz, "Hypoxic/ischemic models in newborn piglet: comparison of constant FiO_2 versus variable FiO_2 delivery," *Brain Research*, vol. 1100, no. 1, pp. 110–117, 2006.

[16] M. Abed, A. Belouchrani, M. Cheriet, and B. Boashash, "Time–frequency distributions based on compact support kernels: properties and performance evaluation," *IEEE Transactions on Signal Processing*, vol. 60, no. 6, pp. 2814–2827, 2012.

[17] S. Dong, M. Mesbah, B.E. Lingwood, J.M. O'Toole, and B. Boashash, "Time–frequency analysis of heart rate variability in neonatal piglets exposed to hypoxia," *Computing in Cardiology*, vol. 38, pp. 701–704, 2011.

[18] S. Dong, F. Xu, B. Lingwood, M. Mesbah, and B. Boashash, "R-wave detection: a comparative analysis of four methods using newborn piglet ECG," in *10th International Conference on Information Sciences Signal Processing and their Applications (ISSPA),* pp. 320–323, 2010.

[19] B. Boashash and T. Ben-Jabeur, "Design of a high-resolution separable-kernel quadratic TFD for improving newborn health outcomes using fetal movement detection," in *11th International Conference on Information Science, Signal Processing and their Applications (ISSPA),* pp. 354–359, 2012.